NASA Technical Memorandum 83372

A Variable-Geometry Combustor Used to Study Primary and Secondary Zone Stoichiometry

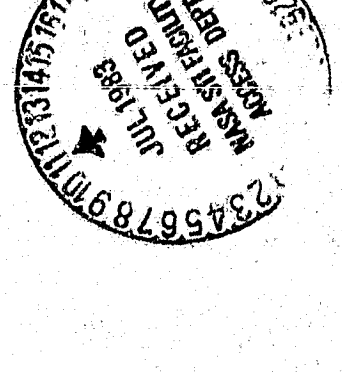

Daniel Briehl, Donald F. Schultz,
and Robert C. Ehlers
Lewis Research Center
Cleveland, Ohio

Prepared for the
Joint Power Generation Conference
sponsored by the American Society of Mechanical Engineers
Indianapolis, Indiana, September 25-29, 1983

NASA

A VARIABLE-GEOMETRY COMBUSTOR USED TO STUDY PRIMARY AND SECONDARY ZONE STOICHIOMETRY

Daniel Briehl, Donald F. Schultz,
and Robert C. Ehlers

National Aeronautics and Space Administration
Lewis Research Center
Cleveland, Ohio 44135

ABSTRACT

A combustion program is underway to evaluate fuel quality effects on gas turbine combustors. A rich-lean variable geometry combustor design was chosen to evaluate fuel quality effects over a wide range of primary and secondary zone equivalence ratios at simulated engine operating conditions. The first task of this effort, was to evaluate the performance of the variable geometry combustor. The combustor incorporates three stations of variable geometry to control primary and secondary zone equivalence ratio and overall pressure loss. Geometry changes could be made while a test was in progress through the use of remote control actuators. The primary zone liner was water cooled to eliminate the concern of liner durability.

Emissions and performance data were obtained at simulated engine conditions of 80 percent and full power. Inlet air temperature varied from 611 to 665 K, inlet total pressure varied from 1.02 to 1.24 MPa, reference velocity was 18.0 m/sec and exhaust gas temperature was a constant 1400 K.

INTRODUCTION

A great deal of work has been done on the effects of broadened property fuels on aircraft combustor performance (1-4). However, this work has all been done on conventional fixed geometry hardware, which limits the scope of these results. Fixed geometry hardware by its nature limits the range of primary and secondary zone equivalence ratios and the overall pressure loss to narrow limits. Thus, extensive parametric evaluation of primary zone and secondary zone equivalence ratios with different fuels becomes prohibitively expensive. Therefore, an existing variable geometry combustor was selected for this program. This combustor consisted of a water cooled primary zone and three stations of variable geometry to control primary and secondary zone equivalence ratios and overall pressure loss. This hardware was previously successfully used on a ground power research application where steam cooling was employed in the primary zone (5). The water cooled primary zone eliminated the durability problems usually associated with rich-lean combustion of nitrogenous fuels. Reference 6 found that nitric oxide emissions were not a strong function of wall temperature thus water cooling has a small impact on results.

The results reported are part of a larger effort which will utilize the variable geometry combustor to explore stoichimetric effects on performance using broadened specification fuels. The results reported are from the preliminary phase of this larger program. In addition to the stoichimetric variations possible with this combustor, two different primary zones were tested in order to evaluate the effects on performance of primary zone residence time.

Emissions and performance data were obtained at conditions simulating a 12:1 pressure ratio engine from 80 percent to full power. Inlet air temperature varied from 611 to 665 K, inlet pressure varied from 1.02 to 1.24 MPa, reference velocity was 18.0 m/sec and exhaust gas temperature was a constant 1400 K.

APPARATUS

Variable Geometry Combustor

This combustor was designed so that very high primary zone equivalence ratios could be obtained. The primary zone was water cooled to eliminate local lean zones which would occur along the walls if film cooling was used. A drawing of the combustor is shown in Fig. 1. The combustor shown in Fig. 1 has the larger volume primary zone installed. The primary zone stoichiometry was controlled by varying the vane angle of a variable pitch vane, axial flow swirler located at the inlet to the primary zone. Being a nonfilm cooled liner, the only way air entered the primary zone was either through the swirler or through the air passage of the single air-assist fuel nozzle which penetrated into the primary zone through the center of the swirler. The secondary zone stoichiometry was controlled by circumferentially rotating a band which would open or close the quench holes located at the inlet to the secondary zone. The overall pressure loss was controlled and maintained constant

by circumferentially rotating a band which would open or close the dilution holes located at the inlet to the tertiary zone.

Figure 1 shows the locations of the combustion zones and the variable geometry provisions. This figure also shows that this combustor is a composite of discrete pieces of hardware, i.e., the primary, secondary and tertiary or dilution zones. The housing in which the combustor was mounted had a diameter of 35.6 cm and was 76 cm long. Two different primary zone volumes were used in order to determine the effects of primary zone residence time on combustor performance. The primary zone volumes, their percent of total combustor volume, and the combustor maximum heat release rates are given in table I. Table II lists other characteristic parameters of this combustor.

The combustor was constructed of Hastelloy-X for all the surfaces in contact with the flame. The secondary and tertiary zones were coated on the hot gas side with a thermal barrier coating consisting of an undercoat of 0.127-mm NiAlY and an overcoat of 0.4-mm ZrO_2 $8Y_2O_3$. A shroud was fitted around the secondary and tertiary zones to increase the backside convective cooling by increasing the local air velocity. Type 304 stainless steel was used for the secondary and tertiary shrouds and the exterior of the water cooling jacket for the primary zone.

Water for cooling was introduced on the backside of the primary zone liner at its downstream end where it was manifolded into a narrow 0.33 cm annular channel. This channel extended along the backside of the liner at constant height until it reached the front end of the primary zone where the water was collected for delivery out of the primary zone casing. Twenty 0.32-cm wires divided the water into 20 spiral flow passages within the annular channel. During hot operation, thermal expansion of the Hastelloy-X inner liner would cause the gap between the wires (attached to the Hastelloy-X) and the outer cooler stainless steel shell to diminish to zero clearance, effectively dividing the water flow into 20 spiral passages. These 0.32-cm wires spiraled one-half revolution around the surface of the inner liner.

A DeLavan air assist fuel nozzle Model 32163 was used for all the testing. Figure 1 shows such a nozzle installed. All of the testing was done using Jet A fuel.

Test Facility

A closed duct, high pressure, nonvitiated test facility was utilized for this program. Test conditions simulating idle to full power could be obtained.

The combustion rig is shown schematically in Fig. 2. In operation air is metered and then enters an indirect fired preheater where the air is heated to the desired temperature. Upon heating the air entered an inlet plenum where the combustor inlet temperature and pressure were measured. Fuel, air assist nozzle air, and primary zone water cooling lines all share this plenum downstream of the inlet instrumentation station. The variable geometry combustor used a 35.6 cm diameter by 1.51 cm thick housing. This relatively large size pipe was necessitated by the variable geometry actuation mechanism and by the water cooling line plumbing. An exhaust instrumentation section followed the test section. Remote control valves were used upstream and downstream of the rig to provide flow and pressure control.

Liner Instrumentation

Twenty-one Chromel-Alumel thermocouples were installed to monitor liner temperatures, eight on both the primary and secondary zone and five on the tertiary zone. A static pressure tap was also located in each combustion zone to provide pressure drop information for calculating airflow into each zone.

Exhaust Instrumentation

Exhaust instrumentation consisted of 40 platinum vs platinum-13-percent-rhodium thermocouples mounted 5 to a rake on centers of equal areas. There were 8 of these rakes. Static pressure taps, and a 10 point centers-of-equal-area gas sample probe completed the exhaust instrumentation. Their location is shown in Fig. 2. The gas collected from all 10 ports of the gas sample probe was passed to a common manifold and from there through steam-heated lines to a gas analysis console. The exhaust gas was analyzed for concentration of CO_2, CO, unburned hydrocarbons, oxide of nitrogen and smoke in accord with the recommendations set forth in Refs. 7 and 8.

PROCEDURE

Combustor Operation

Operation of the combustor was accomplished by setting desired primary zone and secondary zone equivalence ratios for each test point. This was done by adjusting the position of the swirler vanes until the desired primary zone equivalence ratio was achieved. This equivalence ratio was based on the sum of the airflows through the swirlers and the air-assist fuel injector. Secondary zone equivalence ratio was then set by adjusting the secondary zone variable area holes until the desired airflow in the secondary zone was achieved. Secondary zone equivalence ratio was calculated using the sum of the airflows from the primary zone, the variable area secondary zone holes, and secondary zone film cooling holes. As far as it was possible the overall pressure drop of the entire combustor was kept constant by varying the area of the tertiary zone holes.

Flow Calibration

In order to be able to determine equivalence ratio in each combustion zone of this multiple zone variable geometry combustor, it was necessary to flow calibrate each zone while its variable geometry component was cycled. This calibration was accomplished in three stages, one for each combustion zone. For convenience, the secondary zone was calibrated first. To calibrate the secondary zone it was assembled into the combustor housing with the following modifications to prevent air from entering into the primary and tertiary zones: (1) The swirler assembly was removed from the primary zone and a blank-off plate installed thus preventing air from entering; (2) A dam was installed at the junction of the secondary and tertiary zone; (3) The tertiary zone shroud was plugged and the tertiary zone shroud auxiliary holes were taped closed.

The secondary zone calibration utilized near ambient pressure and temperature air. The calibration began with the secondary zone variable geometry holes in the closed position. Airflow was then measured as combustor differential pressure was varied from three to nine percent in three percent increments. The actuator that controlled the position variable geometry in the secondary zone was then moved to 10 percent of its travel and data on airflow and combustor differential pressure were taken. This process was repeated until the entire actuator range from full closed to full open was completed. Check points were

taken on the return to full close position to determine repeatability and to verify that the flow was independent of the direction of actuator travel.

Once the secondary zone actuator was returned to the closed position, the tertiary zone was unplugged. The flow-pressure drop matrix used to calibrate the secondary zone was repeated for each tertiary zone actuator position. The secondary zone actuator remained closed while the tertiary zone actuator was varied. The actual tertiary zone airflow was then obtained by subtracting the calculated secondary zone airflow which was based on the secondary zone flow calibration, from the total airflow which was feeding both the secondary and tertiary zones. During tertiary zone calibration, the primary zone remained blocked off.

The primary zone variable area swirler was flow calibrated by itself using the same flow-pressure drop procedure for each different vane angle. From these data, curves of effective discharge coefficient at constant pressure differential versus actuator position for each swirler assembly were obtained. These curves were then used to obtain airflows entering each combustor zone.

Test Conditions

Operating conditions representative of a 12:1 pressure ratio engine were chosen. Table III lists the conditions which ranged from 80 percent to full power. A limited amount of data was also taken at 30 and 50 percent power levels. At the 30 and 50 percent power condition only liner temperature data is presented.

RESULTS AND DISCUSSION

Exhaust Emissions

Nitric Oxide Emissions. Figures 3(a) to 3(c) show oxides of nitrogen (NO_x) emission index as a function of primary zone equivalence ratio. These data are for two different size primary zones as shown in table I. For the large volume primary zone, both climb-out and take-off power conditions are plotted. For the small volume primary zone only the climb-out power condition is given. In all cases, secondary zone equivalence ratio is presented as a parameter.

Figure 3a represents the 80 percent power point with the small volume primary zone. For the cases where the secondary zone equivalence ratios were 0.58 and 0.43, there is a downward trend in emissions of NO_x as the primary zone equivalence ratio is increased. The minimum NO_x emissions are found at the highest values of primary zone equivalence ratios. It would appear from these data that to achieve the minimum NO_x emissions, a secondary zone equivalence ratio of 0.43 or less should be used along with a primary zone equivalence ratio of at least 1.5.

Data on NO_x emissions for the large volume primary zone is shown on Figs. 3(b) and 3(c). In Fig. 3(b) it is apparent that NO_x emissions are not a strong function of primary zone equivalence ratio. As in the previous case, minimum NO_x emissions require secondary zone equivalence ratios as low as possible. Levels of NO_x emissions with the large volume primary zone are similar to the average levels observed at the 80 percent power condition with the small volume primary zone. The same comments applied to Fig. 3(b) apply to Fig. 3(c). Residence times are higher with this larger volume primary zone. Hot residence time is about 10 ms for the large volume primary zone and about 5 ms for the small volume primary zone.

Figure 4 is a plot for the small and large volume primary zones showing only the secondary zone equivalence ratio that produced minimum NO_x. The secondary zone equivalence ratio producing minimum NO_x for both zones was the lowest value tested, i.e., 0.43 for the small volume and 0.40 for the large volume primary zone. The two curves converged at the higher values of primary zone equivalence ratio. It is conceivable that if it were possible to obtain leaner values of secondary zone equivalence ratio, NO_x emissions might have been lower. Leaner values of secondary zone equivalence ratio were not possible with the experimental hardware because of the limits in the size of the variable area quench holes.

Carbon Monoxide Emissions. Figures 5(a) to 5(c) shows carbon monoxide (CO) emission index as a function of primary zone equivalence ratio. The plots are for 2 different primary zone volumes as outlined in table I. For the large volume primary zone, both climb-out and take-off power data are plotted. For the small volume primary zone only the climb-out power data are given. Secondary zone equivalence ratio is again presented as a parameter.

Figure 5(a) shows that CO emissions generally increase with increasing primary zone equivalence ratio for both secondary zone equivalence ratios tested. However, for a secondary zone equivalence ratio of 0.43, CO emissions peak at a primary zone equivalence ratio of about 1.5. Low values of CO emissions were obtained at less rich primary zone equivalence ratios (between 1 and 1.5). If richer primary zone equivalence ratios are desired (greater than 1.5), minimum CO would be obtained at a secondary zone equivalence ratio of 0.43.

Figure 5(b) presents CO emissions as a function of primary zone equivalence ratio for the large volume primary zone at 80 percent power. At a secondary zone equivalence ratio of 0.40, there is a peak in the CO concentrations at a primary zone equivalence ratio of about 1.3. For a secondary zone equivalence ratio of 0.44 CO emissions are virtually insensitive to the primary zone equivalence ratio. Thus if a primary zone equivalence ratio operating point above 1.6 is chosen, secondary zone equivalence ratios of both 0.40 and 0.44 will give low values of CO emissions. It should be noted that small changes in secondary zone equivalence ratios can cause large changes in combustor performance.

For the same configuration as Fig. 5(b), Fig. 5(c) presents CO emissions at the full power conditions. As with the previous figure, a secondary zone equivalence ratio of 0.41 produced maximum CO sions. In order to obtain minimum CO emissions a secondary zone equivalence ratio of 0.44 was required. The emissions data at a secondary zone equivalence ratio of 0.50 was midway between the curves at 0.41 and 0.44. Also, as with the previous figure, the data at a secondary zone equivalence ratio of 0.41 was a stronger function of primary zone equivalence ratio, being a maximum at a primary zone equivalence ratio of 1.2. At secondary zone equivalence ratios of 0.50 and 0.44, CO emissions were not a very strong function of primary zone equivalence ratio.

Unburned Hydrocarbon Emissions. Emissions of Unburned hydrcarbons were less than 1 part per million (ppm).

Smoke Emissions. Smoke emissions were high. These high smoke emissions are thought to be due, at least in part, to the fuel injection technique employed. Specifically, a poor exhaust temperature profile at all operating conditions indicated a maldistribution of fuel within the combustor and consequently the need for improvement in fuel preparation. Other fuel injection technqiues are currently being investigated in an effort to minimize smoke emissions.

Combustion Efficiency. Combustion efficiency was determined by exhaust gas analysis. As shown in the Exhaust Emission section, all of the combustion inefficiency is attributable to carbon monoxide since less than 1 ppm of hydrocarbon was present. It is quite apparent from examinatior of Figs. 4 and 6 that the large volume primary zone section significantly outperformed the small volume primary zone section. The large primary zone section had combustion inefficiencies on the order of 0.1 percent at primary zone equivalence ratios of 0.8 and 1.65, while the small primary zone section inefficiencies ran from 0.2 to 1.4 percent at the same equivalence ratios.

Hydrocarbon emissions were less than one ppm for all points tested was mentioned earlier. Therefore, resulting inefficiecy due to hydrocarbons was be less than 0.003 percent. The large volume primary zone section produced combustion efficiencies in excess of 99.8 percent when operated at selected points and still exceeded 99.7 percent when operated at any primary zone equivalence ratio from 0.8 to 1.65. Another type of inefficiency in this combustor is cycle inefficiency due to the loss of heat through primary zone water cooling. There was approximately two percent cyclic inefficiency due to this heat loss.

Combustor Durability. A nonconventional technique (a water cooled primary liner) was employed to enhance primary zone liner durability. In cycling from lean-rich equivalence ratios in the primary zone and back as would be encountered in the parametric study this program requires, it is necessary to maintain the liner temperature below 800K to avoid carbonization of the liner material. Carbonization can cause the liner to fail in just a few rich-lean cycles. Figure 7 shows the maximum liner temperature to be about 480K and that liner temperature was independent of equivalence ratio. As expected, figure 8 shows that liner temperature were found to decrease with decreasing power levels. Maximum temperature of the film cooled secondary and tertiary liners remained within acceptable levels.

At the 30 and 50 percent power condition only liner temperature data is presented. Air swirler resonance was encountered during operation of the combustor during these low power conditions. Because of this resonant condition, operations at low power were avoided. The combustor resonant conditions were severe enough to cause failure in the swirler vanes. These vanes have since been redesigned for the follow-on efforts planned for the hardware.

Total pressure loss. Figure 9 is a plot of hot flow total pressure loss as a function of axial length for the variable geometry combustor at the full power condition. Pressure drop across the diffuser was not included. Most of the pressure drop was taken across the variable geometry air swirler to promote rapid mixing in the rich-burn primary zone. It was intended that the next largest pressure drop should occur at the quench plane. Obviously this did not occur. Secondary zone liner film cooling air was found to be excessive. Unfortunately this reduced the amount of air available for quenching the primary zone products while maintaining a particular secondary zone equivalence ratio. Secondary zone film cooled liner temperatures at the full power conditions ranged from 750 to 1100 K, as opposed to the design temperature of 1200 K.

SUMMARY OF RESULTS

As the initial phase of an effort to determine the effects of fuel properties on primary zone and secondary zone combustor stoichiometry, a variable geometry combustor was studied using Jet A fuel. This combustor utilized water cooling to maintain rich-burn primary zone combustor liner integrity. The rich-burn primary zone was followed by a lean-burn secondary zone and a tertiary or dilution zone. Two different volume primary zones were tested. Among the results were:

1. Doubling the volume of the primary zone gave a reduction of NO_x for a range of primary zone equivalence ratios with secondary zone equivalence ratio at an optimum value.
2. The large volume primary zone had minimum NO_x at a secondary zone equivalence ratio of 0.41 and primary zone equivalence ratios greater than 1.4.
3. The large volume primary zone performed with a significant reduction CO in exhaust emissions when compared to the smaller volume primary zone. Combustion efficiency remained acceptable (>99.5 percent) over a range in primary zone equivalence ratios from 0.8 to 1.65.
4. Liner durability was satisfactory and the variable geometry parts performed well except for the primary zone variable area swirler.

REFERENCES

1. Cohen, J. D., "Analytical Fuel Property Effects - Small Combustors (Phase 1)," R82AEB078, General Electric Comp., Lynn, MA, Apr. 1983. (NASA CR-168138).
2. Taylor, J. R., "Analytical Evaluation of the Impact of Broad Specification Fuels on High Bypass Turbofan Engine Combustors," R79AEG504, General Electric Co., Cincinnati, OH, Aug. 1979. (NASA CR-159641).
3. Fear, J. S., "NASA Broad-Specification Fuels Combustion Technology Program: Status and Description," NASA TM-79315, 1979.
4. Butze, H. T., and Humenik, F. M., "Parametric Performance of a Turbojet Engine Combustor Using Jet A and Diesel Fuel," NASA TM-79089, 1979.
5. Schultz, D. F., "Techniques for Enhancing Durability and Equivalence Ratio Control in a Rich-Lean, Three-Stage Ground Power Gas Turbine Combustor," NASA TM-82922, 1982.
6. Russell, P., Beal, G. and Hinton, B., "Low NO_x Heavy Fuel Combustor Concept Program," GTR-3236, United Technologies Corp., South Windsor, Conn., Oct. 1981. (NASA CR-165512).
7. "Procedure for the Continuous Sampling and Measurement of Gaseous Emissions from Aircraft Turbine Engines," Aerospace Recommended Practice 1256, Oct. 1977, revised June 25, 1980, SAE.
8. "Aircraft Gas Turbine Engine Exhaust Smoke Measurement," Aerospace Recommended Practice 1179, May 4, 1970, revised June 15, 1980, SAE.

TABLE I. - VARIABLE GEOMETRY COMBUSTOR DESIGN DETAILS

Primary zone	Volume, M^3	Percent total volume	Max. heat release rate,[a] joule/hr M^3 MPa
Medium volume	3.32×10^{-3}	30.8	1.36×10^{12}
Large volume	6.49×10^{-3}	46.5	1.05×10^{12}

[a]Based on combustor total volume

Table II. - RESIDENCE TIMES AND EQUIVALENCE RATIO VARIATIONS

Primary zone residence time	3.5 - 10.0 msec
Secondary zone residence time . . .	2.5 - 2.95 msec
Primary zone equivalence ratio	0.6 - 2.0
Secondary zone equivalence ratio	0.45 - 0.55
Total pressure loss	3.0 percent

TABLE III. NOMINAL TEST CONDITIONS FOR VARIABLE GEOMETRY COMBUSTOR

Power level	25 percent	Full
Total airflow, kg/sec	4.9	5.3
Inlet temperature, K	610	665
Inlet total pressure, MPa	1.02	1.21
Inlet mach no.	0.0138	0.0133
Exit average temperature, K	1297	1422
Fuel-air ratio	0.0191	0.0241
Fuel weight flow, kg/sec	0.093	0.114
Reference velocity, m/sec	18.0	18.3

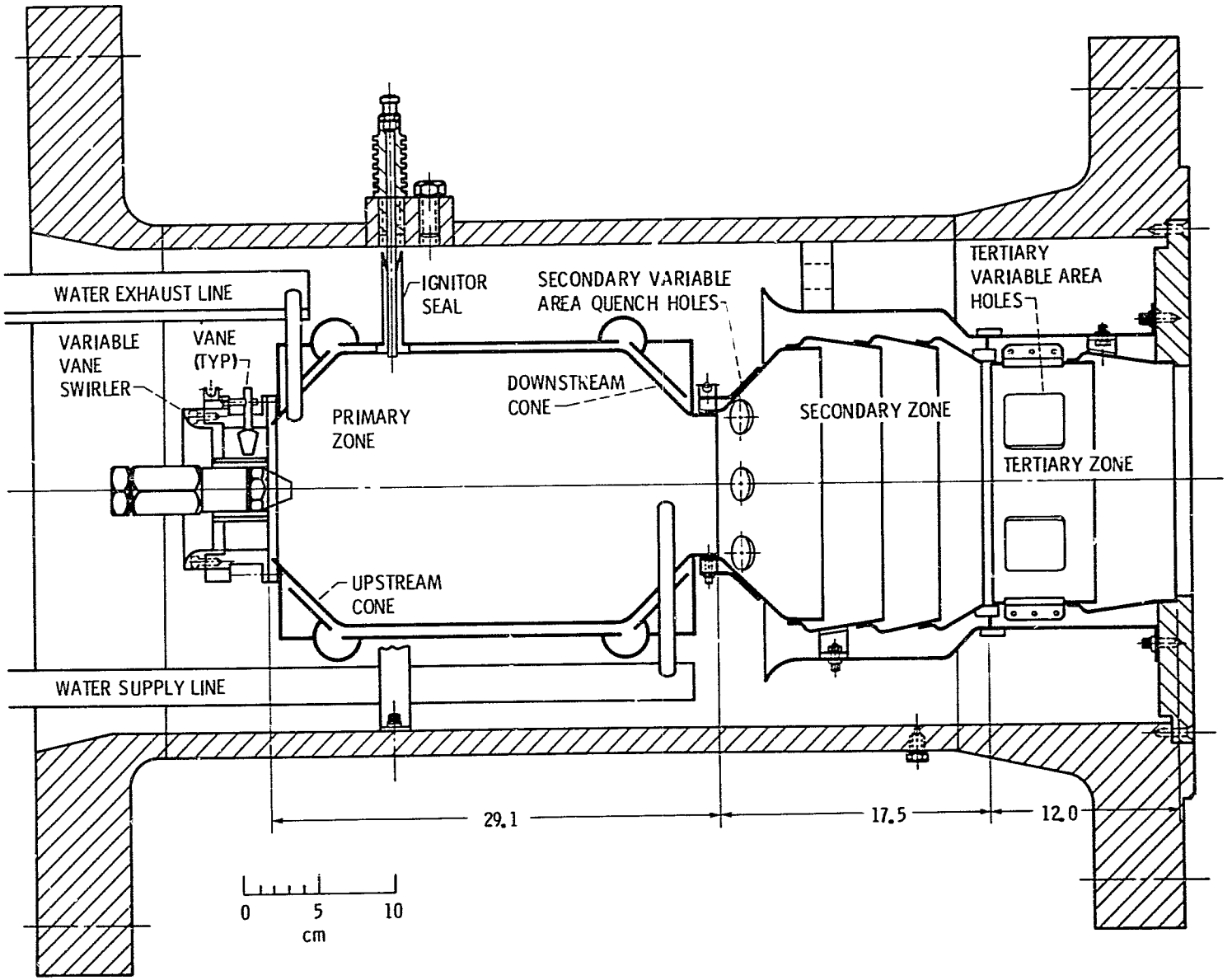

Figure 1. - Cross section of variable geometry combustor with C_3 primary zone, dimensions in centimeters.

CD-82-12925

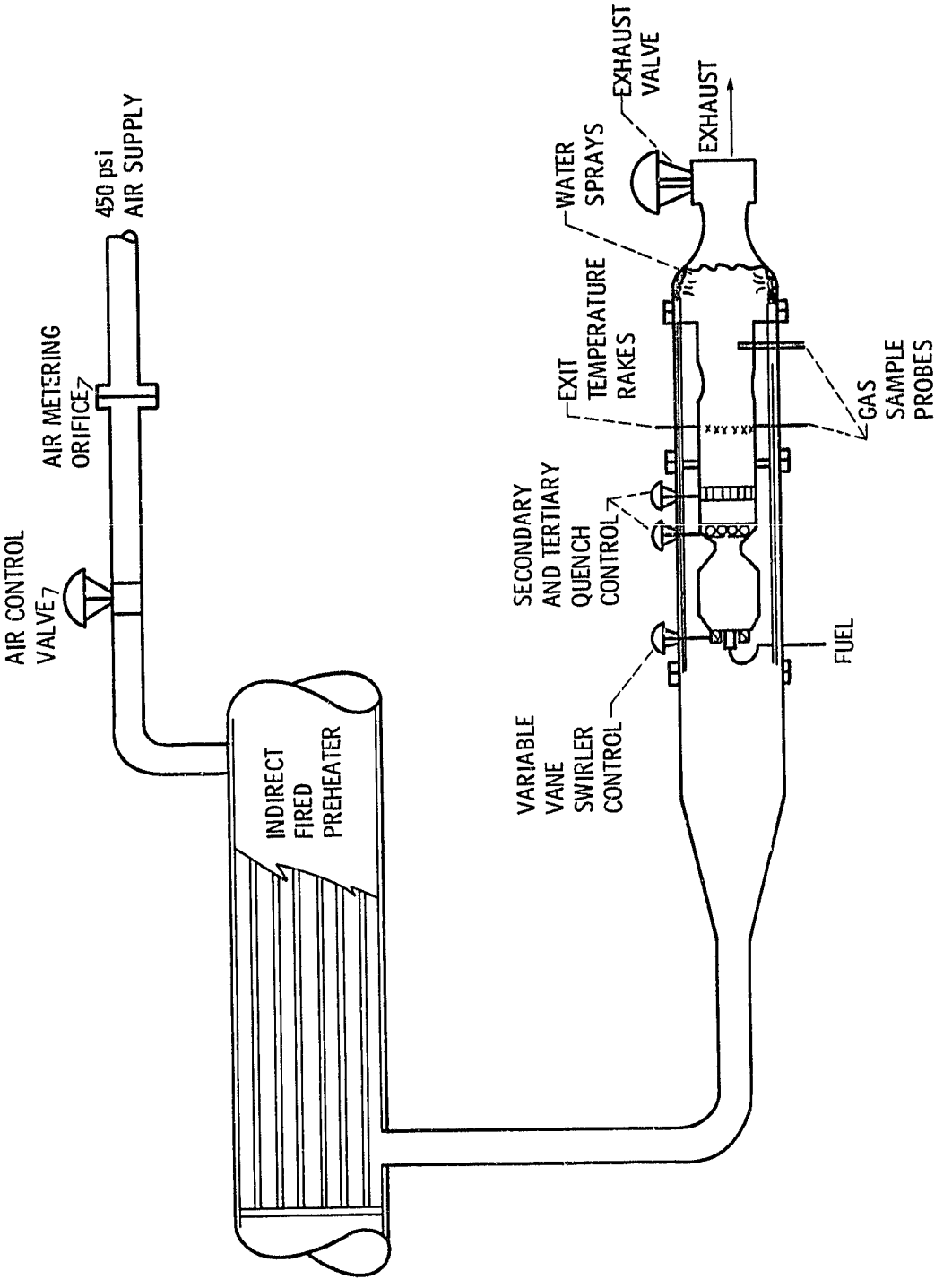

Figure 2. - Schematic drawing of test rig.

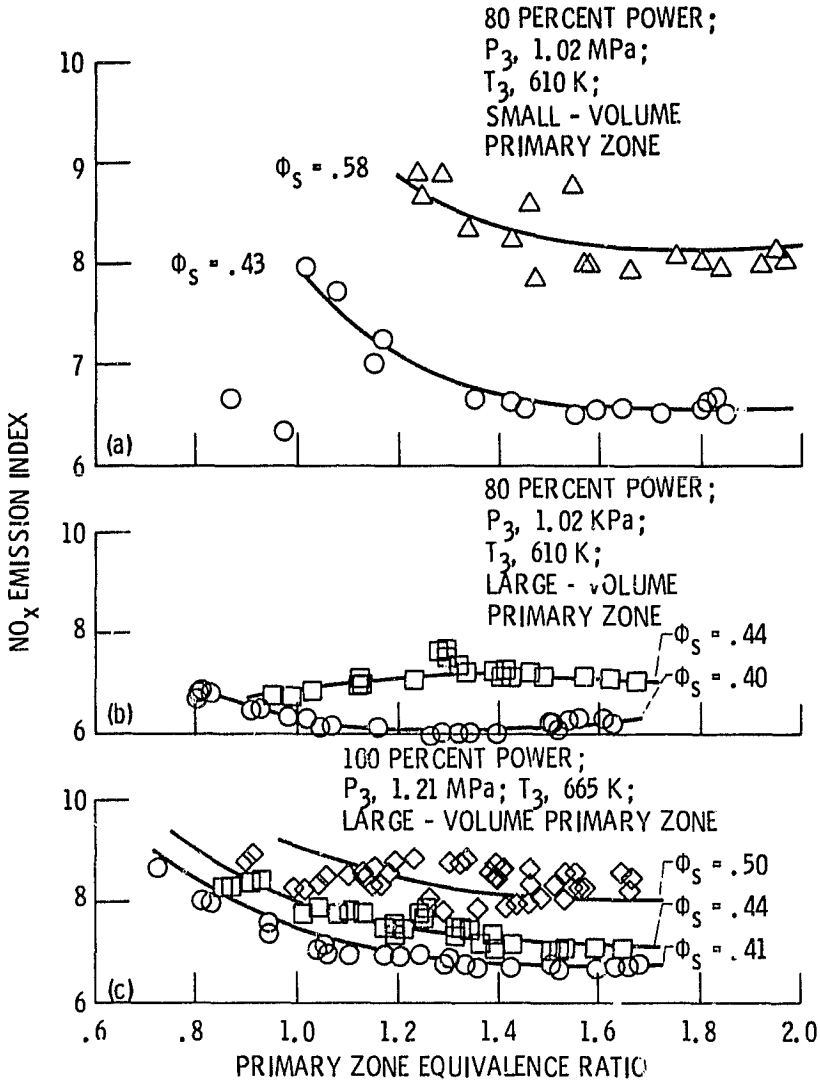

Figure 3. - NO_x emission of a function of primary zone equivalence ratio with secondary zone equivalence ratio as a parameter.

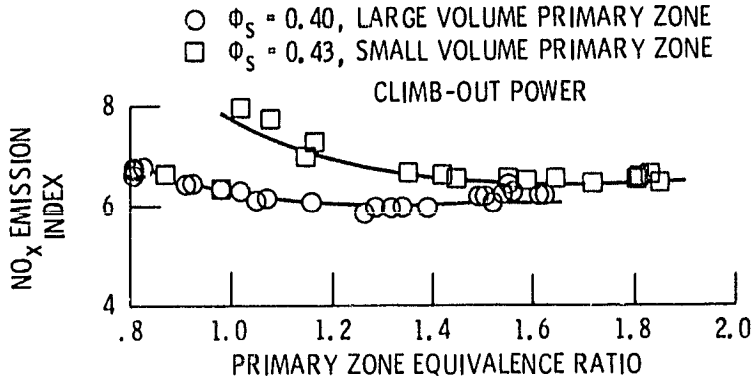

Figure 4. - NO_X emissions as a function of primary zone equivalence ratio for the secondary zone equivalence ratio that produces minimum nitric oxide emissions. Two different primary zone volumes.

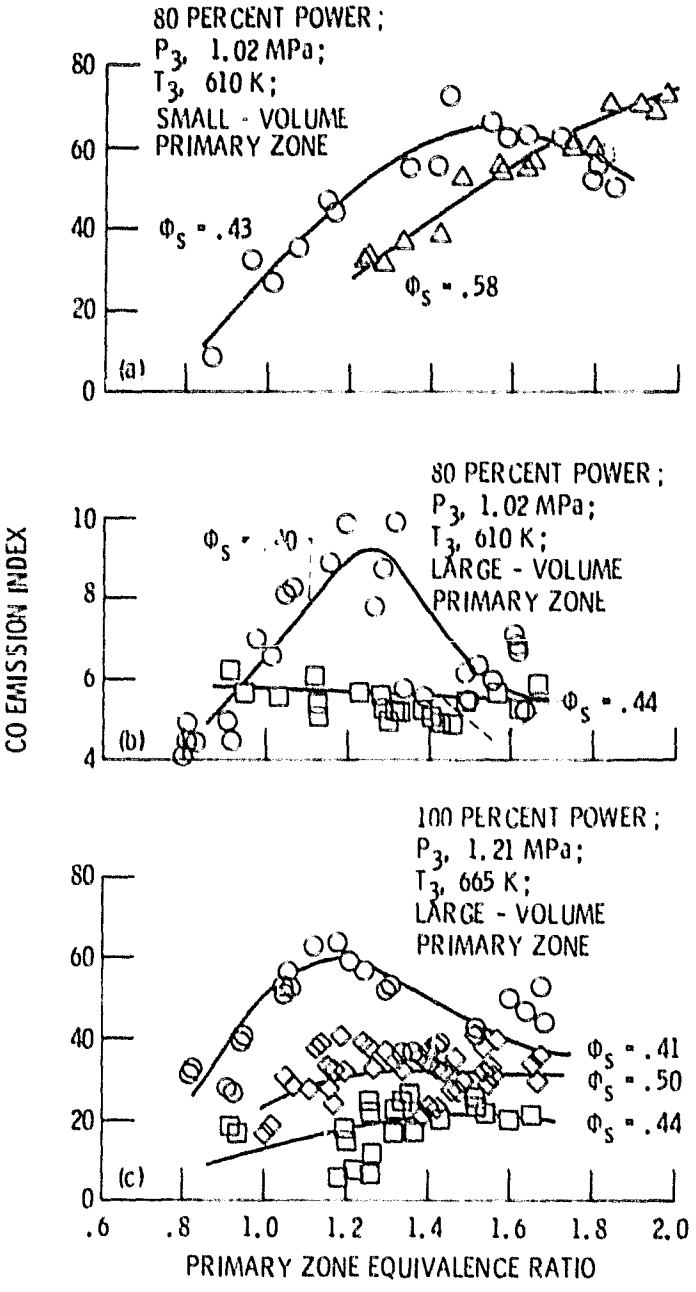

Figure 5. - CO emissions and combustion efficiency as a function of primary zone equivalence ratio with secondary zone equivalence ratio as a parameter.

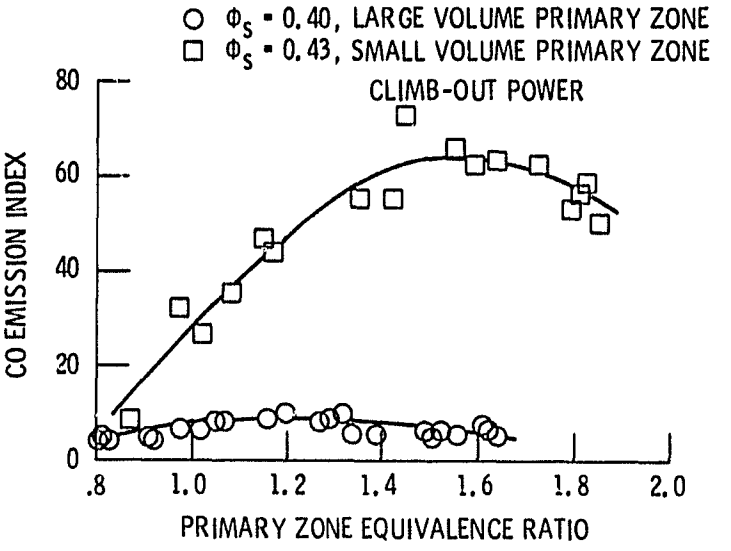

Figure 6. - CO emissions and combustion efficiency as a function of primary zone equivalence ratio for the secondary zone equivalence ratio that produces minimum NO_x emissions. Two different primary zone volumes.

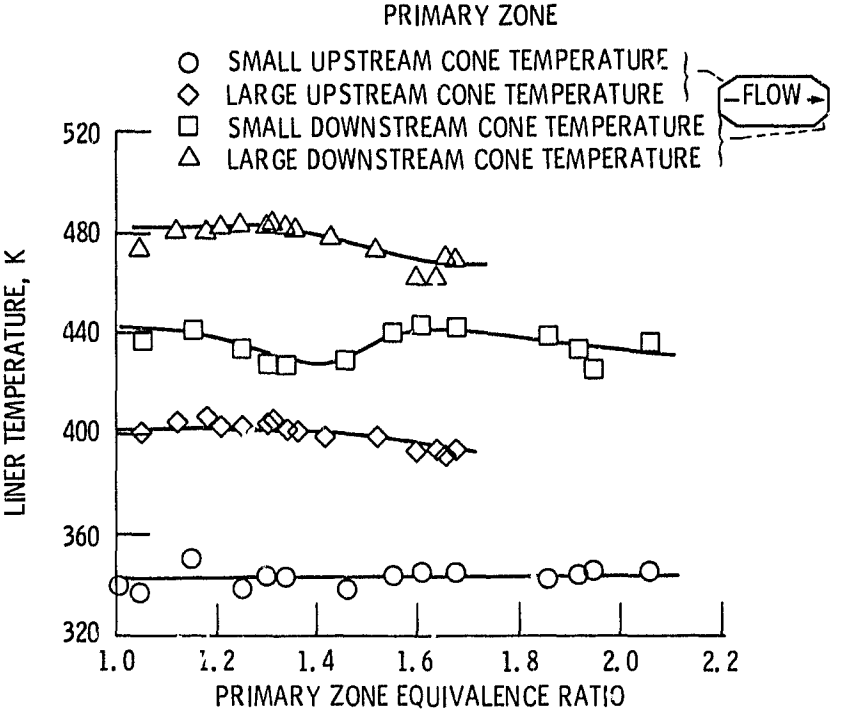

Figure 7. - Primary zone liner temperature as a function of primary zone equivalence ratio at take-off power conditions.

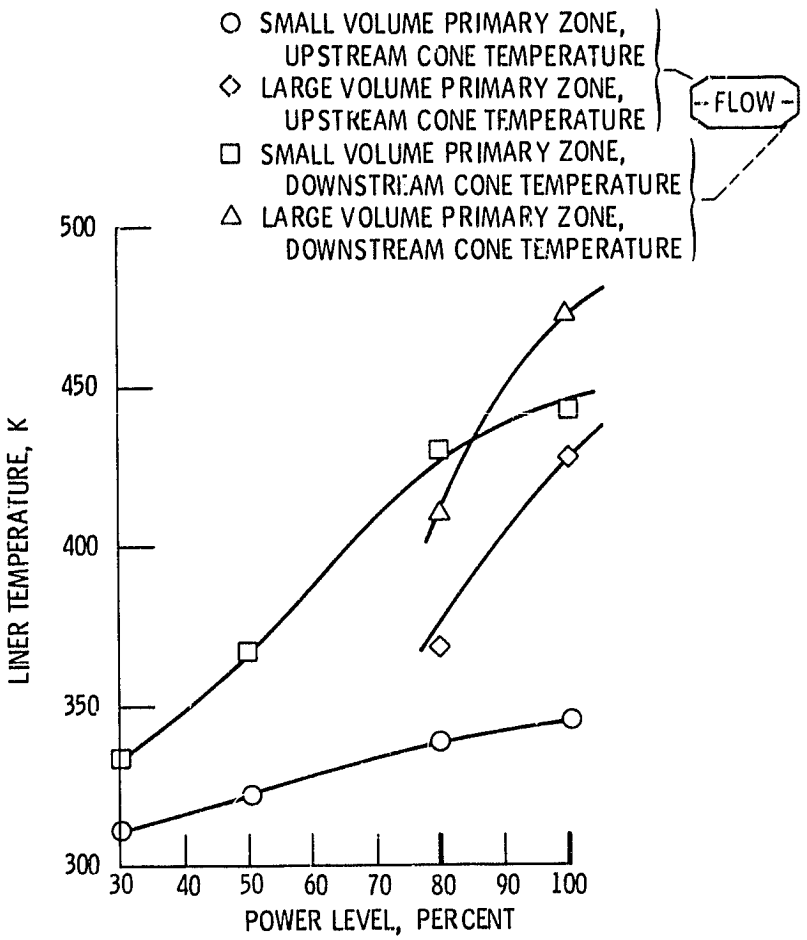

Figure 8. - Primary zone liner temperature as a function of combustor power level.

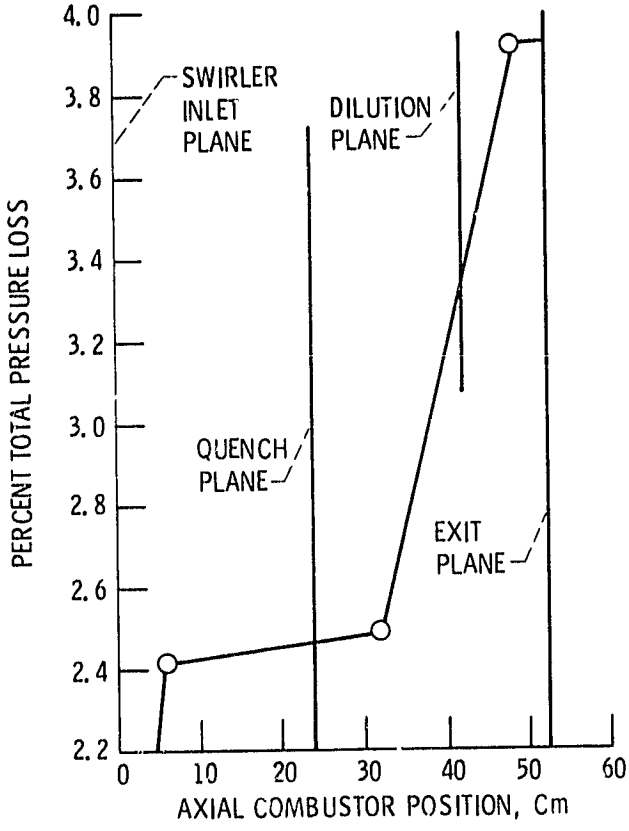

Figure 9. - Variable Geometry Combustor total pressure loss as a function of axial length, 100 percent power condition.